Health and Technology (2020) 10:429–435
https://doi.org/10.1007/s12553-019-00353-0

ORIGINAL PAPER

Multimodal 3D rigid image registration based on expectation maximization

M. J. Velázquez-Durán[1] · D. U. Campos-Delgado[1] · E. R. Arce-Santana[1] · A. R. Mejía-Rodríguez[1]

Received: 31 January 2019 / Accepted: 25 July 2019 / Published online: 29 August 2019

Abstract

Image registration is an important task in medical imaging, capable of finding displacement fields to align two images of the same anatomic structure under different conditions (e.g. acquisition time and body position). Specifically, multimodal image registration is the process of aligning two or more images of the same scene using different image acquisition techniques. In fact, most of the current image registration approaches are based on Mutual Information (MI) as a similarity metric for image comparison; however, the cost function used in MI methods is difficult to optimize due to complex relationships between variables and pixels intensities. This work presents an Expectation Maximization (EM) 3D multimodal rigid registration approach, which introduces a low computational cost alternative with a linear optimization strategy and an intuitive relation among the free variables. Our approach was validated against a state-of-the-art MI-based technique with synthetic T1 MRI brain volumes. The EM 3D achieved a global average DICE index of 96.68 % with a computational time of 22.72 seconds, whereas the MI methodology reported 96.11 % and 35.13 seconds, respectively.

Keywords Expectation maximization · Medical imaging · Multimodal rigid registration · Mutual information

1 Introduction

Each medical image acquisition technique provides a visually different perspective of the same body structure; however, variations in intensity and positions make it necessary to bring the anatomy details acquired with each of these techniques into a common understanding. In this sense, the goal of multimodal image registration in medical imaging is to find a geometrical transformation that properly combines information from two views of the same structure to support specific medical decisions (e.g. disease diagnosis, treatment planning, treatment follow up).

The state of the art in multimodal medical image registration is predominated by Mutual Information (MI) methods [4, 7–9, 13–15]; however, MI cost functions lack an intuitive relationship among the free variables. Moreover, they usually require complex optimization methods with local optima and intensive numerical calculations. Consequently, the images and cost functions are continuously subsampled. In this sense, the Expectation Maximization (EM) technique is a viable alternative to compare multimodal information at a low computational cost and considering the comprehensive relationship between pixels intensities and variables. From this perspective, the goal of this work is to propose a multimodal 3D rigid registration approach based on the EM strategy to be used in medical imaging.

The rest of the work is organized as follows. In Section 2, we propose the cost function of our EM registration method. Similarly, we describe the scenario for the synthetic comparison between an MI-based approach and our EM strategy, using images from the BrainWeb database [6]. Section 3 introduces the comparison results and their discussion in terms of time and precision. Finally, in Section 4, we present our research conclusions.

✉ M. J. Velázquez-Durán
mvelazquez_17@hotmail.com

D. U. Campos-Delgado
ducd@fciencias.uaslp.mx

E. R. Arce-Santana
arce@fciencias.uaslp.mx

A. R. Mejía-Rodríguez
aldo.mejia@uaslp.mx

[1] Facultad de Ciencias, Universidad Autonóma de San Luis Potosí, San Luis Potosí, México

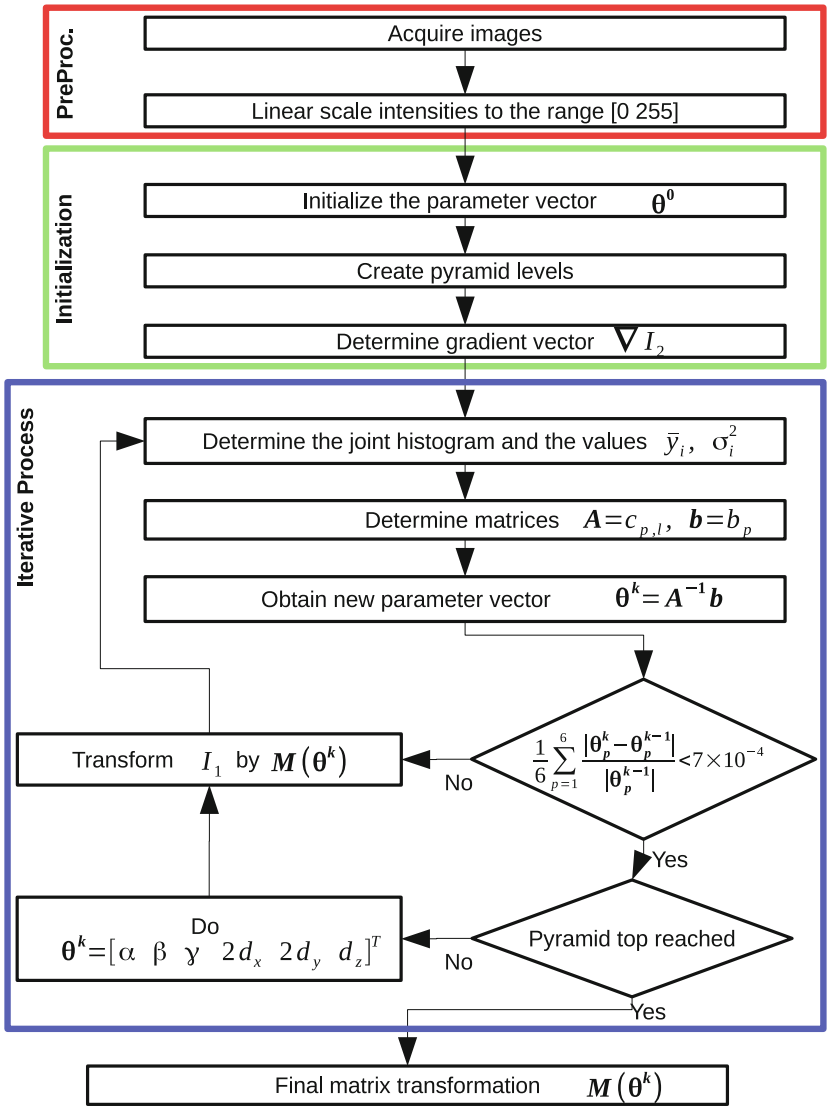

Fig. 1 Block diagram of the EM rigid registration method, where k index represents the iteration number

2 Methods

2.1 EM cost function

In medical imaging, a given body structure can show different tonalities or intensity variations, depending on the image acquisition technique that is used. Therefore, selecting the right similarity metric in multimodal image registration is a crucial task [10].

The EM algorithm provides a multimodal similarity between two images with different intensity distributions each, as follows in [1]. Let I_1 and I_2 be two volume images

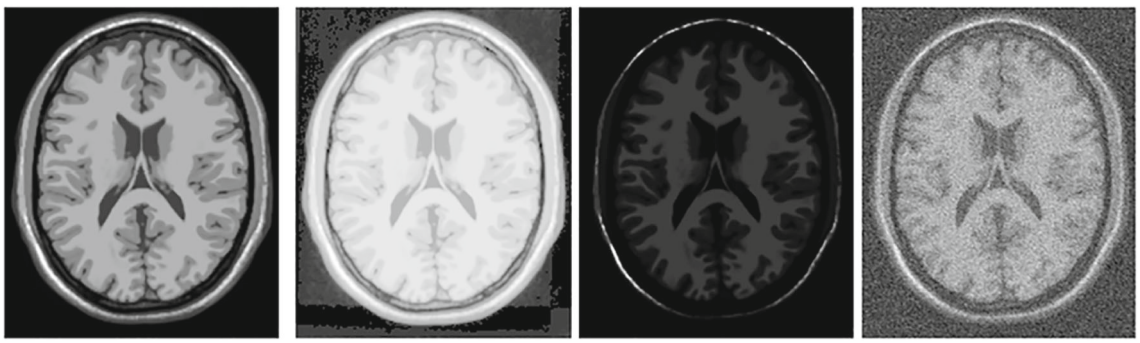

Fig. 2 Examples of the 2D slices of the transformed volumes: original image, $\gamma = 0.25$, $\gamma = 4$ and noise 9%, from left to right

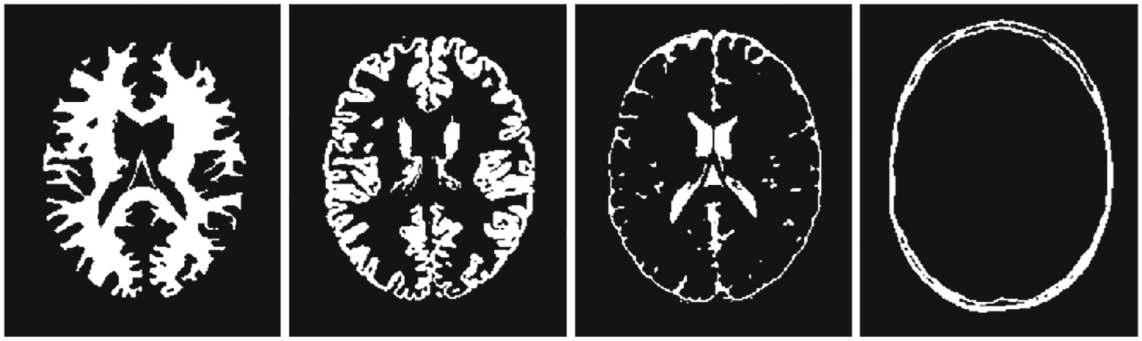

Fig. 3 Examples of anatomical structure used for DICE index: white matter, gray matter, cerebrospinal fluid and skull, from left to right

to be compared in terms of their pixels intensities. For a given intensity value in I_1, the spatial related distribution of intensities in I_2 is calculated and assumed as Gaussian. In the i-th voxel, the mean intensity ($\overline{y}_i$) is used as the comparable value between images I_1 and I_2, and variance ($\overline{\sigma}_i$) gives a confidence weight for the cost function in Eq. 1 introduced by [2]:

$$Q(\boldsymbol{M}(\boldsymbol{\theta})) = \frac{1}{2}\sum_{\boldsymbol{i}\in\mathcal{L}} \frac{[y_i - I_2(\boldsymbol{M}(\boldsymbol{\theta})\boldsymbol{i})]^2}{\sigma_i^2} \tag{1}$$

where $\boldsymbol{\theta} = [\alpha, \beta, \gamma, d_x, d_y, d_z]^T$ is the parameters vector in the 3D rigid transformation (three rotation angles and three displacements), $\boldsymbol{i} = [x, y, z, 1]^T$ the voxel homogeneous coordinates, $\boldsymbol{\mathcal{L}}$ is the voxel coordinates lattice, and $\boldsymbol{M}$ is the rigid transformation matrix.

Using the first-order Taylor approximation formula in the transformed image, we have:

$$I_2(\boldsymbol{M}\boldsymbol{i}) \approx I_2(\boldsymbol{i}) - \nabla I_2(\boldsymbol{i})^T\boldsymbol{i} + \nabla I_2(\boldsymbol{i})^T\boldsymbol{M}\boldsymbol{i}, \tag{2}$$

and with $\Delta I(\boldsymbol{i}) = \overline{y}_i - I_2(\boldsymbol{i}) + \nabla I_2(\boldsymbol{i})^T\boldsymbol{i}$, the cost function in Eq. 1 is then transformed into:

$$Q(\boldsymbol{M}(\boldsymbol{\theta})) = \sum_{\boldsymbol{i}\in\mathcal{L}} \frac{1}{2\sigma_i^2}[\Delta I(\boldsymbol{i}) - \nabla I_2(\boldsymbol{i})^T\boldsymbol{M}\boldsymbol{i}]^2 \tag{3}$$

In the EM algorithm, the $\boldsymbol{M}$ rigid transformation matrix is represented by a parametric structure as follows:

$$\boldsymbol{M} = \boldsymbol{M}_0 + \sum_{p=1}^{n} \boldsymbol{\theta}_p\boldsymbol{M}_p \tag{4}$$

with $n = 6$ as the number of free parameters, $\boldsymbol{M}_0$ as a fixed matrix, and $\boldsymbol{M}_p$ as a constant matrix representing the contribution of each parameter to the rigid transformation $\boldsymbol{M}$. Assuming small rotation angles (α, β, γ) around the axis (x, y, z), the rigid transformation matrix $\boldsymbol{M}$ can be represented as follows:

$$\boldsymbol{M} = \begin{pmatrix} 1 & -\gamma & \beta & d_x \\ \gamma & 1 & -\alpha & d_y \\ -\beta & \alpha & 1 & d_z \\ 0 & 0 & 0 & 1 \end{pmatrix} \tag{5}$$

Finally, the optimal conditions for the cost function Q in (3) are derived by $\frac{\partial Q}{\partial \theta_p} = 0,\ \forall p \in \{1, ..., n\}$ as indicated below:

$$\sum_{\boldsymbol{i}\in\mathcal{L}} \left[\nabla I_2(\boldsymbol{i})^T \left\{\boldsymbol{M}_0 + \sum_{l=1}^{n}\theta_l\boldsymbol{M}_l\right\}\boldsymbol{i} - \Delta I(\boldsymbol{i})\right] \frac{\nabla I_2(\boldsymbol{i})^T\boldsymbol{M}_p\boldsymbol{i}}{\sigma_i^2} = 0 \tag{6}$$

which is equivalent to the following simplified representation:

$$\sum_{l=1}^{n} \theta_l c_{p,l} = b_p \tag{7}$$

where $c_{p,l}$ and b_p mean the following:

$$c_{p,l} = \sum_{\boldsymbol{i}\in\mathcal{L}} \frac{1}{\sigma_{y_i}^2} \nabla I_2(\boldsymbol{i})^T\boldsymbol{M}_l\boldsymbol{i}\nabla I_2(\boldsymbol{i})^T\boldsymbol{M}_p\boldsymbol{i}$$

$$b_p = \sum_{\boldsymbol{i}\in\mathcal{L}} \frac{1}{\sigma_{y_i}^2} \left[\Delta I(\boldsymbol{i}) - \nabla I_2(\boldsymbol{i})^T\boldsymbol{M}_0\boldsymbol{i}\right] \nabla I_2(\boldsymbol{i})^T\boldsymbol{M}_p\boldsymbol{i}$$

thus resulting in a system of linear equations as follows:

$$\underbrace{\begin{bmatrix} c_{1,1} & c_{1,2} & \cdots & c_{1,n} \\ \vdots & \vdots & \ddots & \vdots \\ c_{n,1} & c_{n,2} & \cdots & c_{n,n} \end{bmatrix}}_{\boldsymbol{A}} \underbrace{\begin{bmatrix} \theta_1 \\ \vdots \\ \theta_n \end{bmatrix}}_{\boldsymbol{\theta}} = \underbrace{\begin{bmatrix} b_1 \\ \vdots \\ b_n \end{bmatrix}}_{\boldsymbol{b}}. \tag{8}$$

2.2 EM registration algorithm

In [2], the EM methodology was applied for 2D registration; however, in this work, we propose a 3D extension. The cost function approximation in Eq. 2 motivates the use of an iterative scheme to reach for the optimal parameters,

Table 1 DICE index by anatomical structure (mean ± variance) for the two registration techniques

	WM	GM	CSF	S
EM	98.21 ± 0.55	97.49 ± 0.77	95.82 ± 1.30	95.22 ± 1.80
MI	97.80 ± 0.92	96.94 ± 1.30	94.97 ± 2.10	94.74 ± 2.10

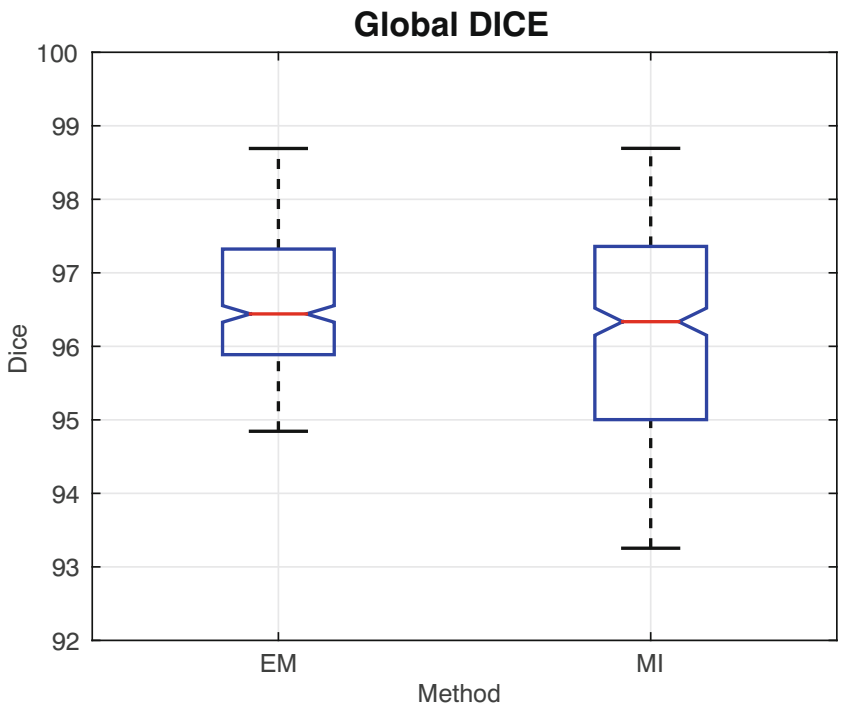

Fig. 4 Global DICE index comparison

similar to a nonlinear least squares strategy. Hence, at each iteration, a 6×6 system of linear equations has to be solved. In addition, the ∇I_2 gradient must be determined at each iteration; however, using a reverse registration method [3], the gradient is only calculated once by transforming I_1 instead of I_2.

Furthermore, the EM registration methodology is performed in a pyramid scale to reach larger transformation ranges and reduce computational time [5] mainly using only the xy plane, since for some volume values, the z plane has limited information. Finally, the stopping criterion (each pyramid level vs precision target) is set to the relative

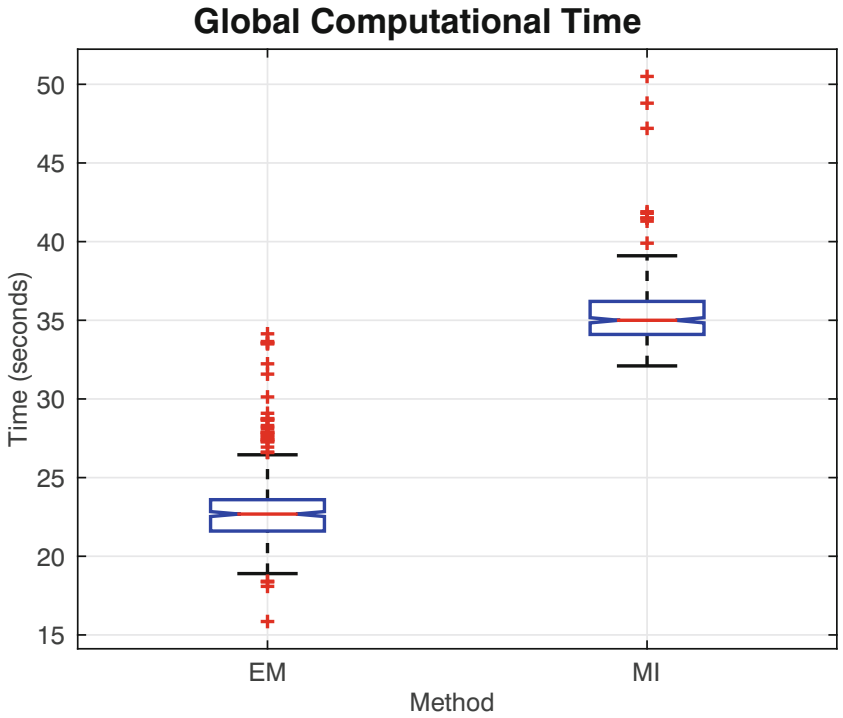

Fig. 5 Global computational time comparison

change in the parameters during the iterative process; this value was set up to 7×10^{-4} by trial and error. The complete block diagram of our EM rigid registration approach is presented in Fig. 1.

2.3 Synthetic evaluation

We performed a synthetic comparison between an MI-based registration algorithm from Elastix [11] and our EM methodology using T1 MRI volumes from the BrainWeb database [6]. Considering that in a real medical scenario the transformations to be recovered usually present a limited range of angles and displacements, the next transformations were generated:

- Rigid: considering rotation angles in ranges 5°, 10°, 15°, 20°, and 25°, and displacements of 5, 10, 15, and 20 mm for each axis.
- Intensity: a nonlinear gamma transformation is applied to normalized intensities i_E by $i_S = i_E^{\gamma}$, and finally re-scaled to the original range, with γ = 1, 2, 4, 0.5 and 0.25, considering that values above 1 darken the image, whereas those below 1 lighten it.
- Gaussian noise: emulating the noise levels used in the BrainWeb database [6], so Gaussian noise was added

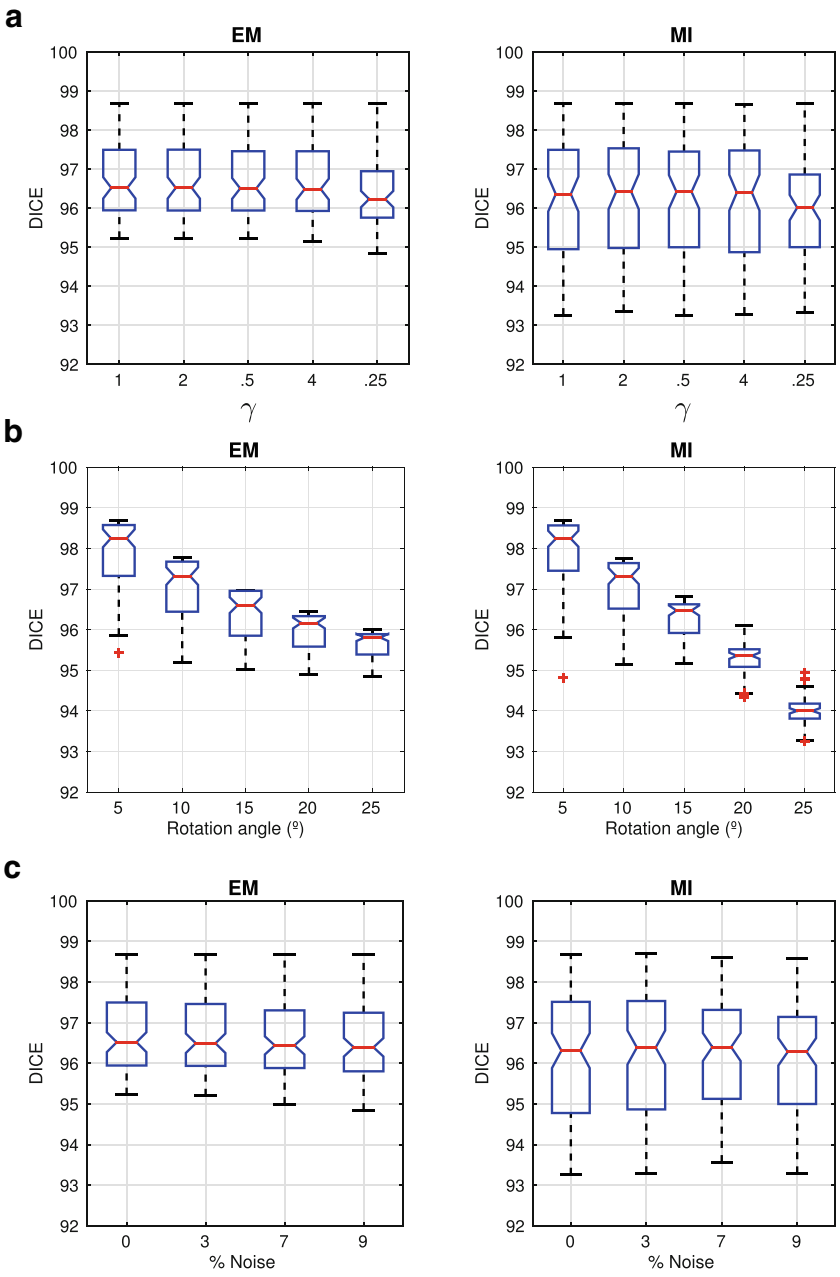

Fig. 6 DICE index against gamma intensity transformation, rotation angle in rigid transformation, and noise level in the synthetic transformations

with variances of 0%, 3%, 7% and 9% of the peak intensity in the image.

In total, we generated 400 random transformations to test each registration method. Some examples of the 2D slices of these transformed volumes are depicted in Fig. 2.

Once the registration process was completed by both methods, we used the ground-truth image to compute the DICE index [12]. Similarly, we calculated computational time to evaluate the performance of each method. The anatomical structures used to obtain the DICE index included: white matter (WM), gray matter (GM), cerebrospinal fluid (CSF), and skull (S). Figure 3 illustrates an example of each of these structures.

3 Results and discussion

Table 1 describes the statistical results (mean ± variance) of the DICE index for each anatomical structure. Notice that a DICE index close to one highlights better registration capabilities. In this sense, the EM methodology outperformed the MI-based methodology during the synthetic evaluation.

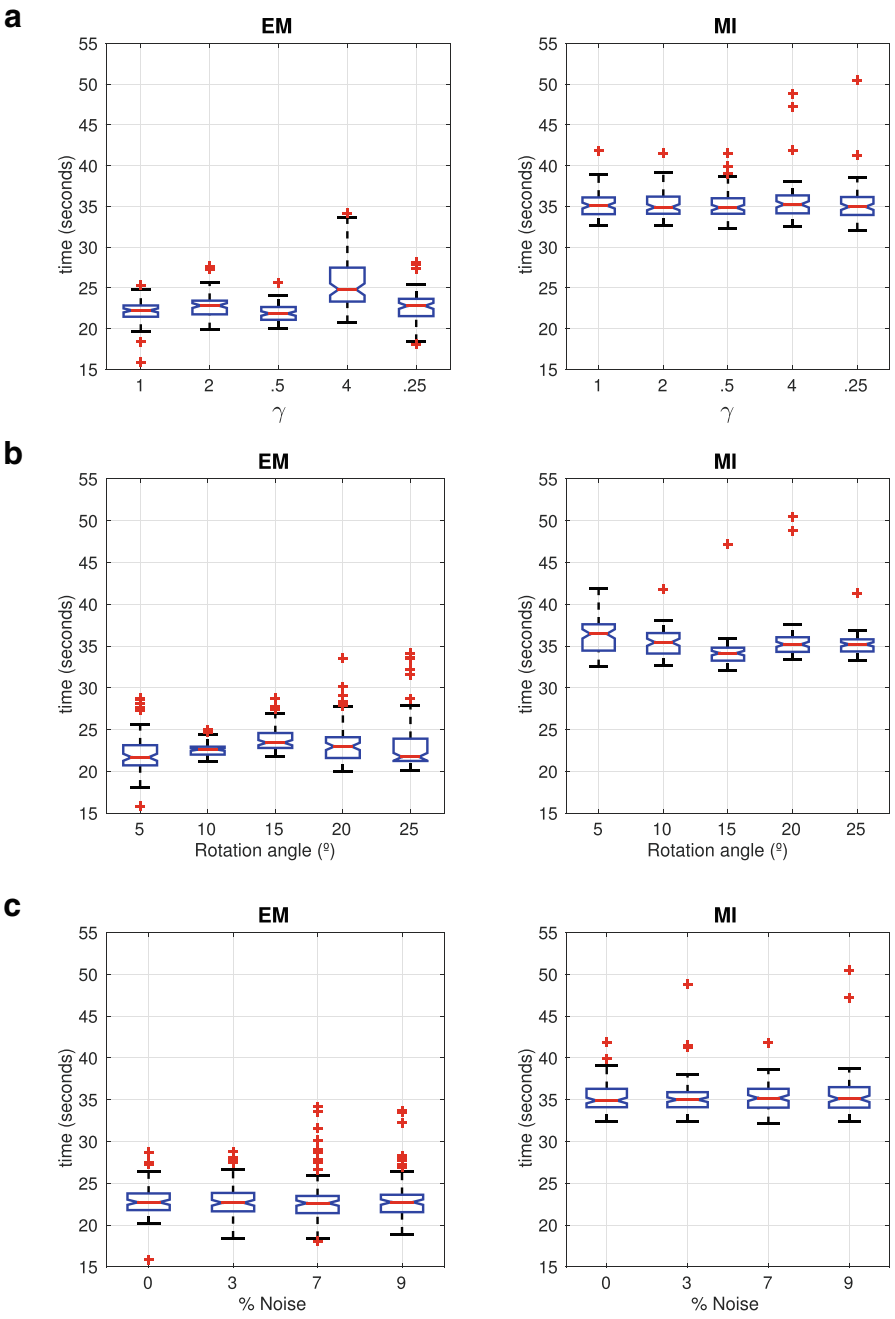

Fig. 7 Computational time against gamma intensity transformation, rotation angle in rigid transformation, and noise level in the synthetic transformations

That is, our approach reported the highest index value and the smallest variance. The box-plot results for the four anatomical structures are introduced in Fig. 4.

With respect to computational time, the EM methodology required shorter execution time than the MI methodology during the synthetic evaluation. Such results are detailed in Fig. 5. Nonetheless, the EM methodology was implemented in MATLAB (a high-level programming language), whereas the MI-based technique from Elastix [11] was executed using C++.

Finally, a marginal analysis (i.e. gamma intensity transformation, rotation angle in rigid transformation, and noise level) was performed with respect to both DICE index and computational time for two methodologies. The results of this analysis are introduced in Figs. 6 and 7. As depicted in Fig. 6, DICE index values decreased as the variation ranges decreased. Meanwhile, as Fig. 7 shows, the computational time remained stable across intensity variations, rotation angles, and noise levels. Furthermore, notice that the EM methodology was computationally faster than the MI-based methodology in all the experiments (i.e. lower computational times, as shown in Fig. 7).

4 Conclusion

During the synthetic evaluation, our EM methodology outperformed the MI-based scheme, achieving a global DICE index of 96.68 % with a computational time of 22.72 seconds —if compared to 96.11 % and 35.13 seconds, respectively, obtained by the MI methodology. As an important advantage, our 3D registration method is independent on volume size by the pyramidal reduction step. Furthermore, to extend the 3D registration scheme, an affine implementation is possible by using a two-step algorithm to keep the transformation matrix as a linear mapping. As future work, a more comprehensive comparison will be pursued over the same programming platform. Nonetheless, the main advantage of our EM technique could be seen in terms of computational time. That is, even though our methodology was implemented in a high-level programming language (i.e. MATLAB), its processing time was shorter than that of the MI-based registration technique, programmed in C++.

Acknowledgements This research was supported by Mexico's National Council of Science and Technology (Conacyt) through a PhD grant number 362210 and a Basic Science project number 254637.

Compliance with Ethical Standards

Conflict of interests The authors declare that they have no conflict of interest.

References

1. Arce-Santana E, Campos-Delgado D, Vigueras-Gómez F, Reducindo I, Mejía-Rodríguez A. Non-rigid multimodal image registration based on the expectation-maximization algorithm. Lect Notes Comput Sci. 2014;8333:36–47.
2. Arce-Santana ER, Campos-Delgado DU, Reducindo I, Mejia-Rodriguez AR. Multimodal image registration based on the expectation–maximisation methodology. IET Image Proc. 2017;11:1246–1253(7). https://digital-library.theiet.org/content/journals/10.1049/iet-ipr.2017.0234.
3. Baker S, Matthews I. Equivalence and efficiency of image alignment algorithms. In: Proceedings of the 2001 IEEE conference on computer vision and pattern recognition, vol 1, pp 1090–1097; 2001.
4. Bron EE, van Tiel J, Smit H, Poot DHJ, Niessen WJ, Krestin GP, Weinans H, Oei EHG, Kotek G, Klein S. Image registration improves human knee cartilage t1 mapping with delayed gadolinium-enhanced mri of cartilage (dgemric). Eur Radiol. 2012;23(1):246–252.
5. Burt PJ, Adelson EH. The laplacian pyramid as a compact image code. IEEE Transactions on Communications. 1983;31:532–540.
6. Cocosco CA, Kollokian V, Kwan RKS, Pike GB, Evans AC. Brainweb: Online interface to a 3d mri simulated brain database. Neuroimage. 1997;5:425.
7. Crum W, Hartkens T, Hill D. Non-rigid image registration: theory and practice. Br J Radiol. 2004;77(SPEC. ISS. 2):S140–S153.
8. de Groot M, Vernooij MW, Klein S, Ikram MA, Vos FM, Smith SM, Niessen WJ, Andersson JL. Improving alignment in tract-based spatial statistics: Evaluation and optimization of image registration. Neuroimage. 2013;76:400–411.
9. Guyader JM, Bernardin L, Douglas N, Poot D, Niessen W, Klein S. Influence of image registration on apparent diffusion coefficient images computed from free-breathing diffusion mr images of the abdomen. J Magn Reson Imaging. 2015;42(2):315–330.
10. Hill DLG, Batchelor PG, Holden M, Hawkes DJ. Medical image registration. Phys Med Biol. 2001;46(3):R1. http://stacks.iop.org/0031-9155/46/i=3/a=201.
11. Klein S, Staring M, Murphy K, Viergever MA, Pluim JPW. Elastix: A toolbox for intensity-based medical image registration. IEEE Trans Med Imaging. 2010;29(1):196–205.
12. Murino V, Puppo E, Sona D, Cristani M, Sansone C. New trends in image analysis and processing – ICIAP 2015 workshops: ICIAP 2015 international workshops, BioFor, CTMR, RHEUMA, ISCA, MADiMa, SBMI, and QoEM, Genoa, Italy, September 7-8, 2015, Proceedings. Lecture Notes in Computer Science. Springer International Publishing. 2015. https://books.google.com.mx/books?id=nKxnCgAAQBAJ.
13. Pluim JPW, Maintz JBA, Viergever MA. Mutual-information-based registration of medical images: a survey. IEEE Transcations on Medical Imaging, pp 986–1004. 2003.
14. Risser LEA. Piecewise-diffeomorphic image registration: Application to the motion estimation between 3d ct lung images with sliding conditions. Med Image Anal. 2012;17(2):182–193.
15. Sotiras A, Davatzikos C, Paragios N. Deformable medical image registration: A survey. IEEE Trans Med Imaging. 2013;32(7):1153–1190.